Analysis of Flow inside Soundproofing Ventilation Unit using CFD

Yuichi Tanaka*, Keisuke Masuda, Norihiro Hayashida, Sohei Nishimura, Teiichi Tanaka

National Institute of Technology, Kumamoto College, Hirayamashin-Machi, Yatsushiro, Kumamoto, 2627, Japan

*Corresponding Author: Yuichi Tanaka, National Institute of Technology, Kumamoto College, Japan.

ABSTRACT

A soundproof window with ventilation has been previously proposed to solve the road noise problem in developing countries in tropical regions. However, a concrete verification method has yet not been established with respect to airflow within the soundproofing ventilation unit (SVU). We studied the airflow inside one such unit using a particle image velocimetry (PIV) system in a previous study. In this investigation, computational fluid dynamics (CFD) analysis results are compared with actual PIV measurements of the flow. The velocity distribution near the outlet of the SVU, displayed in contour forms when an inflow velocity was applied at the inlet, generally reproduced the results of the PIV measurements. The vortex near the upper part of the SVU was also reproducible, confirming that CFD analysis can provide insight into the dynamics of the flow inside the SVU.

Keywords: *Soundproofing Ventilation Unit, Airflow, PIV, CFD*

INTRODUCTION

With the recent economic growth, environmental problems such as road noise are becoming severe in developing countries in tropical regions [1-2]. In general, the use of air conditioners is not common in tropical regions. Instead, casement windows with two sashes that provide good ventilation are widely used. These types of windows, however, are not capable of addressing the issue of the current road noise problem. As a potential solution to the problem, Nasu and Nishimura proposed a soundproof window with ventilation [3]. They performed a 3D analysis of sonic propagation inside a soundproofing ventilation unit and theoretically and experimentally demonstrated noise reduction effects.

However, a concrete verification method has not been established with respect to airflow within the soundproofing ventilation unit. If such a method can be established, it will facilitate the development of a soundproofing ventilation unit with both soundproofing and ventilation characteristics.

We studied the airflow inside a soundproofing ventilation unit (SVU) using a particle image velocimetry PIV system [4]. By measuring the airflow at three different spots of an SVU using PIV, we were able to characterize the airflow distribution inside at each inflow velocity.

Verification of the accuracy of CFD analysis via a comparison with PIV measurements has been reported in previous studies [5-6], and research has also been conducted on the effect of the analysis model and boundary conditions [7].

In this study, an analysis was performed using PIV measurements and computational fluid dynamics (CFD). When investigating the optimal conditions for PIV measurements and comparative verification of the validity of CFD analysis, the goal was to implement an experimental method for performance evaluation of ventilation in an SVU.

OVERVIEW OF SVU USED IN THE ANALYSIS

The external view and dimensions of the SVU used in the CFD analysis are shown in Figure 1. The SVU is equipped with a flow inlet at the bottom surface and a flow outlet on the front surface. The model used in the PIV measurements was made of a 2-mm-thick transparent acrylic resin sheet to enable measurements. A model with the same dimensions was also used in the CFD analysis.

PIV MEASUREMENT OVERVIEW

Figure 2 shows the schematic of the PIV system used to acquire measurements, and Table 1 provides the specifications of the various equipment/instruments used in the investigation [4]. During the measurement process, air mixed

with tracer particles was blown into the model at a constant velocity using a DC fan placed just below the flow inlet.
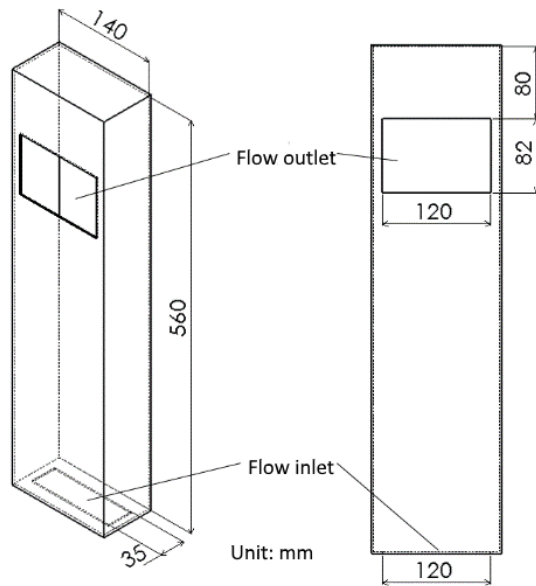
Figure1. *External view of SVU*

The area under measurement was irradiated using a laser, and images of the particle movement were captured using a high-speed camera. The DaVis 8.0 Software was used for velocity analysis and to calculate the 2D cross-sectional velocity vectors.

In the experiments, to confirm the changes caused by the image capture conditions, PIV measurements were conducted by changing the voltage applied to the DC fan (airflow velocity), and the laser pulse interval was appropriately adjusted. The target area for the measurement was set at the centre of the SVU model near the flow outlet. Table 2 summarizes the measurement conditions.
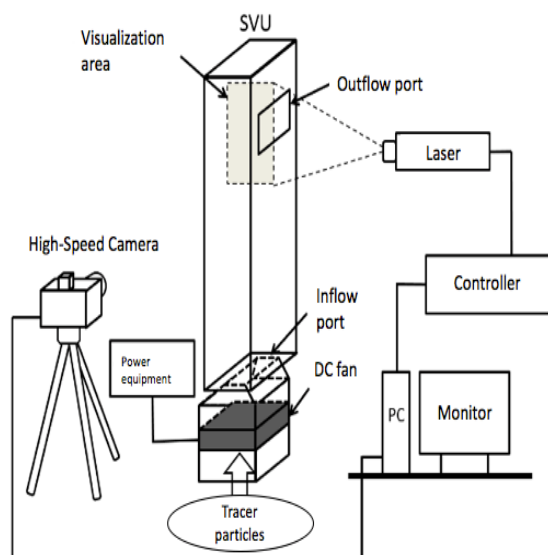
Figure2. *Schematic of PIV system*

Table1. *PIV measurement equipment/instruments*

PIV system	FlowMaster2D-PIV (LaVision GmbH)
Camera	Imager sCMOS
Laser	Double Pulse Nd: YAG Laser
Software	DaVis 8.0 Software
Particle generator	Aerosol Generator
Voltage device	Regulated dc power supply PR18-3A (Kenwood)
DC fan	DC Fan Motor ASFN80372 (Panasonic)
Hot wire anemometer	Anemometer LTE Model 6006 (Kanomax Japan)

Table2. *PIV measurement conditions*

Method	Double frames
Interval	f = 5 Hz
Time	2 s
Investigation window	16×16 pixel, 32×32 pixel
Overlap	75%
Airflow velocity at inlet	6 V, U_{in1} = 0.326 m/s 12 V, U_{in2} = 0.912 m/s 24 V, U_{in3} = 2.025 m/s
Laser pulse interval	200 µs, 500 µs, 800 µs

CFD ANALYSIS OVERVIEW

SOLIDWORKS Flow Simulation 2014 was used in the CFD analysis. In the 3D analysis of internal flow using the k-ε model, the conditions were set as close to the PIV measurement conditions as possible [8].

Rectified airflow was used in the PIV measurements, where the velocity of airflow to the SVU was regulated using the DC fan and flow adjustment flaps. In the CFD analysis, the same airflow velocity was used in the PIV measurements as the boundary condition at the flow inlet. Additionally, assuming natural convection, analysis of the airflow caused by heat generated by a rubber heater was also performed. Although PIV measurements were acquired in experiments using the rubber heater, no significant velocity vector could be obtained because the fluid flow was complex, and therefore, only the results from the CFD analysis are presented in this study.

Table 3 shows a summary of the analysis and boundary conditions when an inflow velocity is applied at the flow inlet. Two types of turbulence parameter, *I-L* and k-ε, can be set at

the flow inlet. In fluid flow, it is often difficult to estimate favourable turbulence in advance. Therefore in this analysis, the values recommended by the SOLIDWORKS Flow Simulation 2014 software were used as the default [9]. To reduce the time needed for the analysis and to evaluate the steady state, a surface goal was set at the flow outlet.

Table3. *Analysis/boundary conditions*

Turbulence parameters	(1) *I-L* (turbulence intensity and length) $I_t = 2\%$, $L_t = 0.0001$ m (2) *k-ε* (turbulence energy and dissipation) $k = 1$ J/kg, $\varepsilon = 1$ W/kg
Number of meshes	27,648
Boundary condition at flow inlet	Velocity (perpendicular to the surface) (1) $U_{in1} = 0.326$ m/s (2) $U_{in2} = 0.912$ m/s (3) $U_{in3} = 2.025$ m/s
Boundary condition at flow outlet	Atmospheric pressure
Boundary condition at wall	Thermally insulated wall, no-slip
Surface goal	Mean velocity at flow outlet

CFD ANALYSIS RESULTS AND COMPARISON WITH PIV MEASUREMENTS

Comparison based on Velocity Distributions

For the CFD analysis and PIV measurements, the velocity distributions along the lines set at the centre of the SVU were compared. Figure 3 shows the position of the lines. Line 1 was set on the xy-plane of the flow outlet, and Line 2 was set as the central horizontal line on the xy-plane at the flow outlet, along which the changes in velocity distribution occur. Line 1 and Line 2 were 82 mm and 70 mm long, respectively.
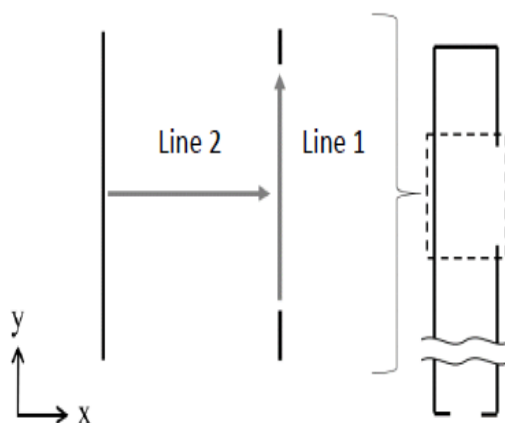
Figure3. *Lines for velocity distribution comparison in SVU*

Figures 4 and 5 show the velocity distributions from the CFD analysis and PIV measurements, which were obtained when a velocity of U_{in1} is applied at the flow inlet. The markers (symbols) show the PIV measurement results at laser pulse intervals of 200 μs, 500 μs, and 800 μs, respectively, whereas the solid and dotted lines show the results of the CFD analysis for turbulence parameters *k-ε* and *I-L*, respectively. The CFD analysis and PIV measurements were conducted with three different velocities applied at the flow inlet, but only the results for U_{in1} are shown.
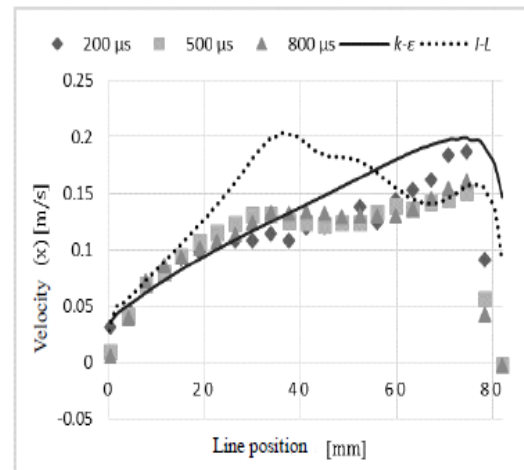
(a) Velocity distribution in the x-direction (U_{in1}) along Line 1
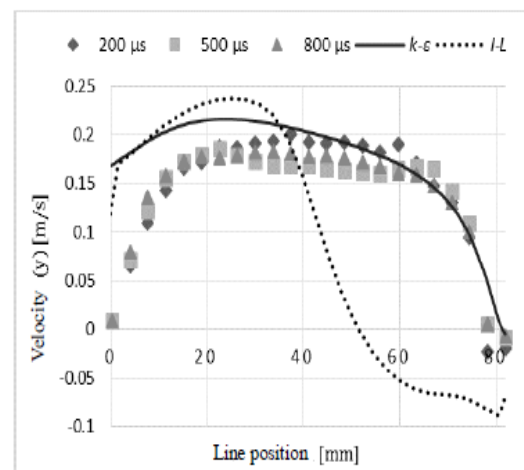
(b) Velocity distribution in the y-direction (U_{in1}) along Line 1

Figure4. *Velocity distribution along Line 1*

For Line 1, Figure 4 (a) shows a comparison of the velocity distribution in the x-direction, and Figure 4 (b) shows a comparison for the velocity distribution in the y-direction.

With respect to the velocity distribution along Line 1 in the x-direction, the values from the *k-ε* model follow the same pattern as the PIV

measurements from 0 mm at the lowest end of the line at the outlet bottom, to approximately 40 mm toward the centre of the outlet. From the centre toward the upper end of the outlet, the values from the k-ε model tend to be higher than those in the PIV measurements. In the case of the I-L model, approximately near the centre region, the values are higher than the PIV values, and unstable velocity changes are observed toward the upper end (beyond the centre).

Regarding the velocity distribution in the y-direction on Line 1, although the velocity at the lower end of the outlet as obtained from the k-ε model tends to be higher than the PIV measurements, the corresponding values appear to reproduce the PIV measurements toward the upper end of the outlet. In the case of the I-L model, below the 40-mm position on the line, although the values are similar to those from the k-ε model, the velocity drops sharply above the centre of the outlet, resulting in a downward flow.

For Line 2, Figure 5 (a) shows the velocity distribution in the x-direction, and Figure 5 (b) shows the distribution in the y-direction.

As shown in Figure 5 (a), the velocity distribution in the x-direction along Line 2 as obtained from the k-ε model, generally reproduces the PIV measurements although they are slightly higher beyond the 40-mm position. In the case of the I-L model, the velocity distribution closely follows the PIV measurements up to approximately the 50-mm position. However, as shown in Figure 5 (a), there is a sharp rise in the velocity near the outlet.

Figure 5 (b) shows that although the velocity distribution in the y-direction along Line 2 as obtained from the k-ε model reproduces the PIV measurements, the distribution obtained from the I-L model is significantly different, resulting in a downward flow.

With respect to the velocity distribution obtained using turbulence parameters, compared with those from the I-L model, the results from the k-ε model were closer to the PIV measurements. In the case of the I-L model, significant differences in the velocity distribution in the y-direction were observed. One likely reason for this may be the effect of the surface goal that was set to judge the steady-state condition. Moreover, because the default values were used for the turbulence parameters, changing these values may have produced different results.
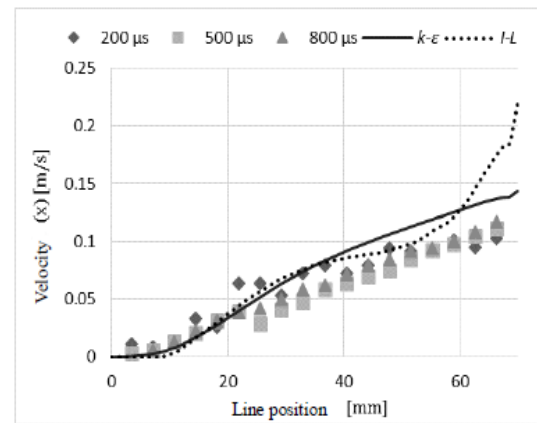
(a) Velocity distribution in the x-direction (U_{in1}) along Line 2
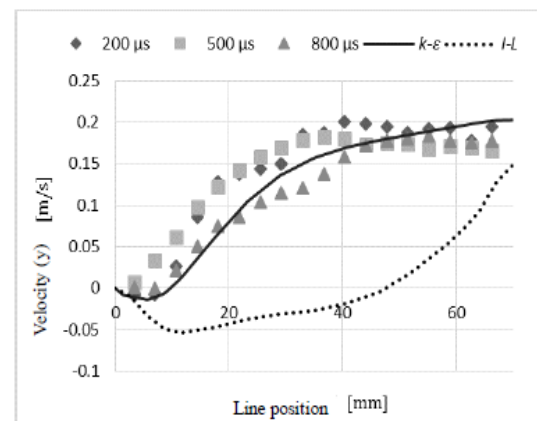
(b) Velocity distribution in the y-direction (U_{in1}) along Line 2

Figure5. *Velocity distribution along Line 2*

Contour-plot-based Comparison of Velocity Distribution in the Vicinity of the Outlet

With respect to the results of the CFD analysis and PIV measurements under the condition of U_{in1} velocity of inflow at the SVU inlet, Figure 6 shows the velocity in the x-direction near the flow outlet, and Figure 7 shows the corresponding velocity in the y-direction using contour plots. The results from CFD analysis with turbulence parameters k-ε, which were in close agreement with the PIV measurements, and the PIV measurements that were obtained using a laser pulse rate of 200 µs are shown in Figures 6 and 7.

The distributions of velocity in the x-direction obtained from the CFD analysis and PIV measurements are almost identical. The velocity in the x-direction is higher near the outlet cross-section and tends to increase near the upper part of the outlet. However, as shown in Figure 4 (a), the velocity values from the CFD analysis are higher and cover a broader range of 0.105 m/s to 0.190 m/s.

For the velocity in the y-direction, the results of the CFD analysis and PIV measurements also exhibit almost identical distributions. The velocity in the y-direction is higher starting from the lower end of the outlet toward the outlet centre. It gradually decreases beyond the centre toward the upper end of the outlet. Both the CFD analysis and PIV measurements confirm the decrease in velocity at the upper end of the outlet.
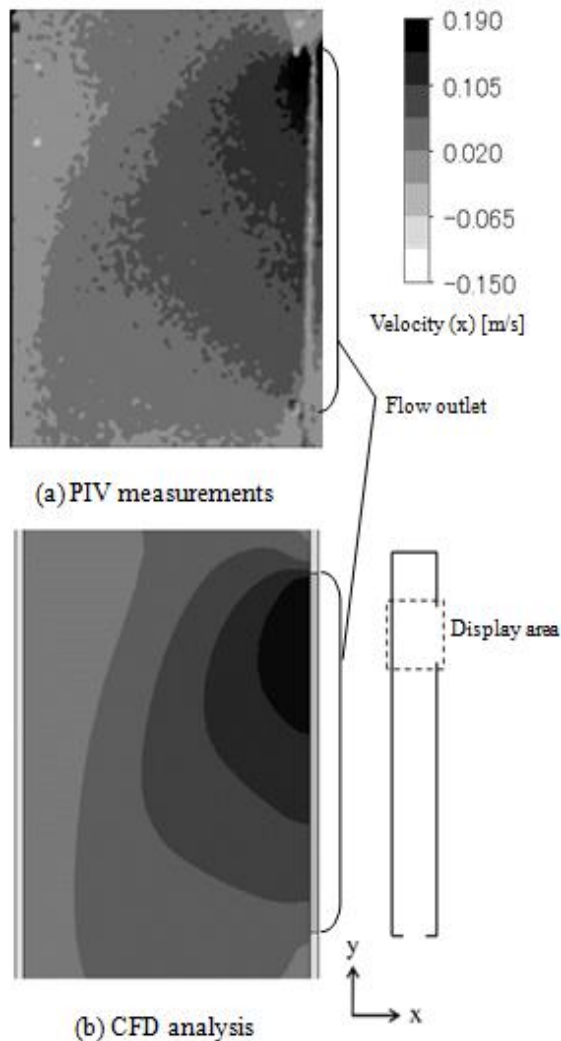
Figure6. *Contour plot of velocity in the x-direction (inflow velocity U_{in1})*

Comparison of Vortex Generation Positions in the Upper Part of the SVU

Figure 8 shows the velocity vector diagram for the upper part of the SVU. The results of using CFD analysis using turbulence parameters *k-ε* and PIV measurements for a laser pulse interval of 800 μs to enable clear identification of the vortex shape, corresponding to an inflow velocity of U_{in1}, are shown here. Similar to the PIV measurements, the CFD analysis results also confirmed the generation of an anti-clockwise vortex in the upper part of the SVU.
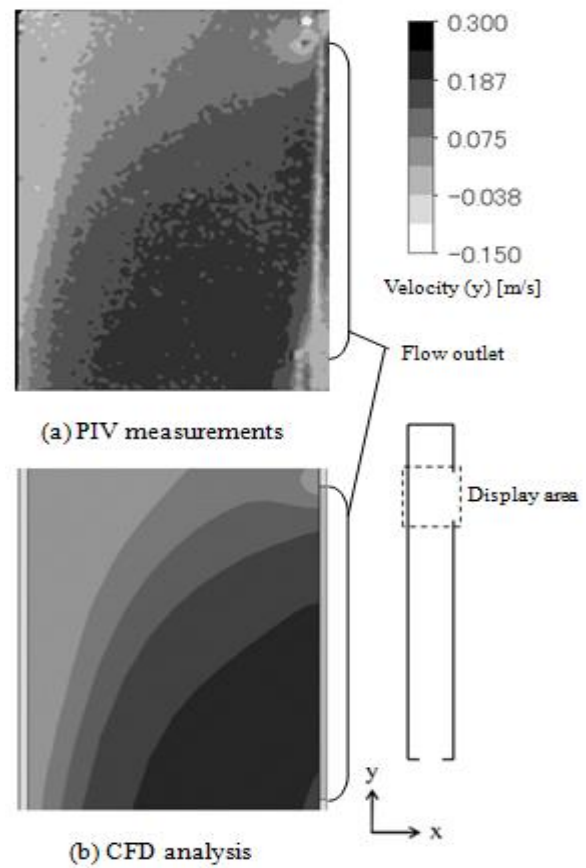
Figure7. *Contour plot of velocity in the y-direction (inflow velocity U_{in1})*
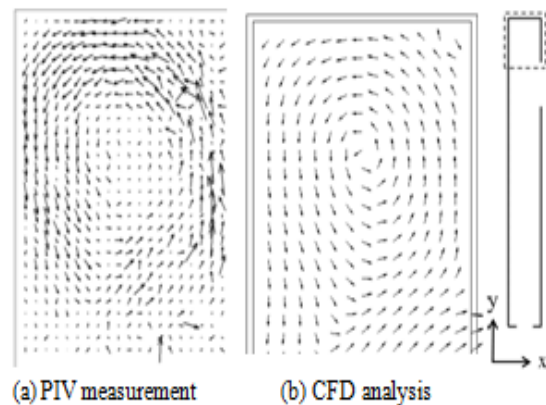
Figure8. *Velocity vector diagram for the upper part of the SVU (inflow velocity U_{in1})*

CFD ANALYSIS OF FLOW INDUCED BY RUBBER HEATER

Assuming the same conditions as in the case of PIV measurements, the CFD analysis of airflow induced by the rubber heater was performed with the SVU, including a case placed at the bottom of the SVU to maintain the tracer particle oil mist.

Figure 9 shows an overview of the model used for analysis. The internal dimensions of the case were as follows: (W × D × H) 300 × 250 × 100 mm, and it was equipped with lateral inlet

openings to let in external air. During the PIV measurements, the oil mist was supplied through a tube placed inside the case. The rubber heater was (W × D) 250 × 200 mm in size and was placed 10 mm below the flow inlet of the SVU.
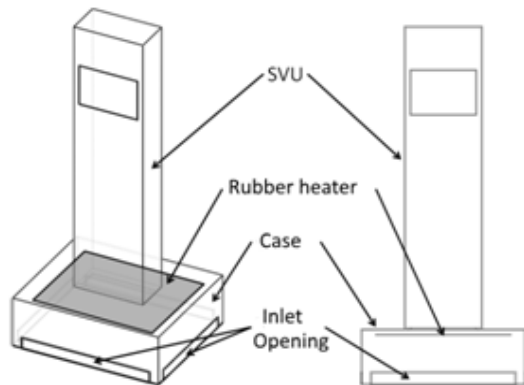
Figure9. *Overview of analysis model for heater induced flow*

Table 4 summarizes the analysis and boundary conditions. The turbulence parameters k-ε were chosen since they generated relatively stable velocity distributions when an inflow velocity was applied, and the rubber heater temperature was set at 40^0.

Figures 10 and 11 shows a comparison of the flow induced by the rubber heater and the flow or an applied flow inlet velocity of U_{in1}.

Although the SVU inflow velocities are different, the rubber-heater-induced flow also differs from the case in which a flow velocity is applied at the inlet, in that the air inflow across the xy-plane moves along and toward the walls in the x-direction, then stagnates at the centre of the upper part of the SVU. Along the yz-plane, the flow under an applied flow inlet velocity of U_{in1} is characterised by generally uniform flow vectors up to a point near the flow outlet, while the flow induced by the rubber heater is also complex in the z-direction.

Table4. *Analysis/boundary conditions*

Turbulence parameters	k-ε, k = 1 J/kg, ε = 1 W/kg
Number of meshes	46,080
Boundary condition at SVU outlet surface	Atmospheric pressure
Boundary condition at case openings	Atmospheric pressure
Wall conditions	Heat insulated wall, no-slip
Surface goal	Mean velocity at outlet cross-section
Rubber heater	Upper surface temperature of 313 K
Outdoor temperature	298 K
Gravity	y-direction, -9.81 m/s^2

(a) Rubber heater   (b) Flow inlet velocity U_{in1}
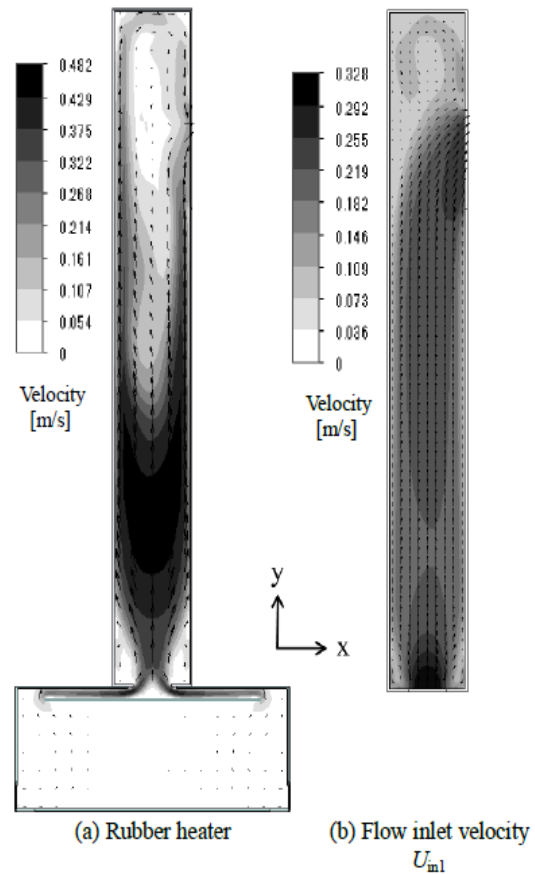
Figure10. *Comparison of rubber-heater-induced flow and flow under applied flow inlet velocity U_{in1} (velocity distribution on xy-plane)*

(a) Rubber heater   (b) Flow inlet velocity U_{in1}
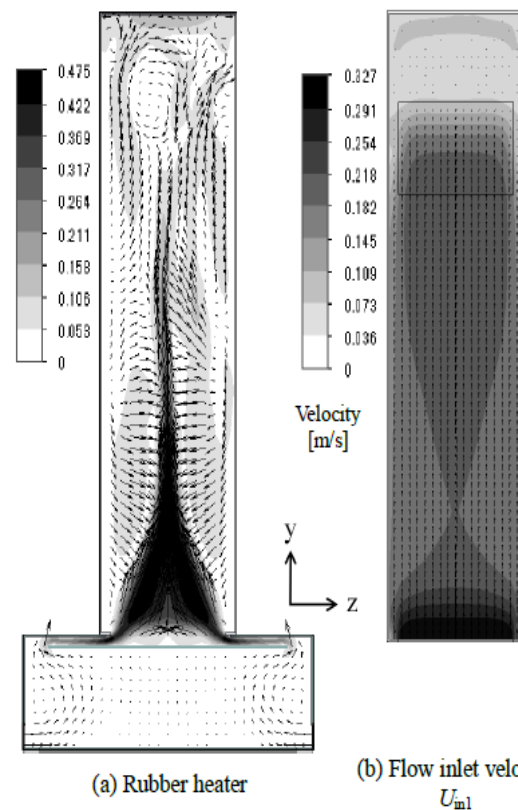
Figure11. *Comparison of rubber-heater-induced flow and flow under applied flow inlet velocity U_{in1} (velocity distribution on yz-plane)*

Figure 12 shows the velocity vectors in the upper part of the SVU. The flow induced by the rubber heater is clockwise, whereas the flow due to an applied flow inlet velocity U_{in1} is anti-clockwise. The flow induced by the rubber heater flows toward the walls of the SVU and moves upward along the left side before flowing out through the outlet, whereas, under the applied flow inlet velocity, the upper part of the flow moving toward the outlet goes up along the right wall and generates a vortex.

(a) Rubber heater   (b) Flow inlet velocity U_{in1}
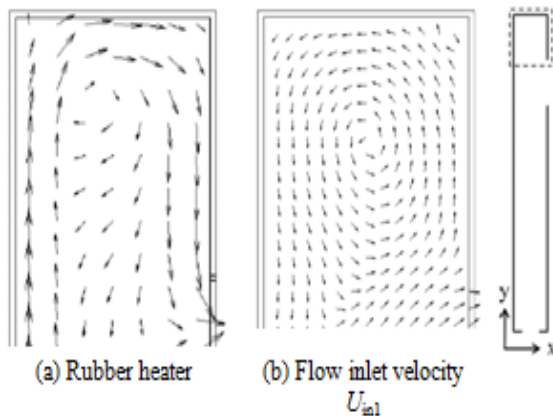
Figure12. *Velocity vector pattern in the upper part of the SVU*

The difference in velocity between the PIV measurements and the CFD analysis may likely be caused by the effects of the flow near the outlet outside of the SVU, which was not considered in the analysis. Expanding the extent of the analysis target for further verification is deemed necessary. Moreover, because unsteady flow and vortex generation may occur, unsteady flow analysis and velocity changes with time also need to be evaluated.

For the PIV measurements in this study, it is necessary to add the presence of tracer particles in the analysis conditions, especially in setting conditions of low inflow velocity because the behaviour of the oil mist used as tracer particles was not taken into account.

With respect to the PIV measurement errors, high accuracy in measurement may not be achieved near the surface of the wall because of reflection of the laser beam. In the upper and lower areas of the SVU outlet with corners, false vectors may appear. This needs to be considered in a comparison of the results.

CONCLUSION

With respect to the flow inside the SVU, CFD analysis results were compared with actual PIV measurements, and the following findings were obtained.

- Although the accuracy of the analysis using turbulence parameters was higher for k-ε than I-L, with the values of k-ε being closer to that obtained via the PIV measurements, differences were also observed in the results obtained with the k-ε model.

- The velocity distribution near the outlet displayed in contour forms under conditions of inflow velocity applied at the inlet generally reproduced the results of the PIV measurements. The vortex near the upper part of the SVU also could be reproduced, confirming that CFD analysis can provide insight into the flow inside the SVU.

- For air flow induced by the rubber heater, the differences in velocity distributions and vortex rotation directions were confirmed based on a comparison with the case in which the inflow velocity was applied at the inlet.

- With respect to differences between the upper and lower part of the SVU outlet, the effects of the flow outside the SVU are likely, which was not considered in the analysis model. Moreover, taking the external flow and unsteady flow into account in future CFD analysis is deemed necessary.

REFERENCES

[1] H. Y. T. Phan, T. Yano, H. A. T. Phan, T. Nishimura, T. Sato, Y. Hashimoto, Community responses to road traffic noise in Hanoi and Ho Chi Minh City, Applied Acoustics, Vol. 71(2), (2010), pp. 107–114.

[2] H. A. T. Phan, T. Yano, H. Y. T. Phan, T. Nishimura, T. Sato, Y. Hashimoto, Annoyance caused by road traffic noise with and without horn sounds, Acoustical Science and Technology, Vol. 30(5), (2009), pp. 327–337.

[3] T. Nasu and T. Nishimura, Acoustic characteristics of a soundproofing unit having an inlet and outlet located on the crossed right angle face, Journal of Environmental Engineering (Transactions of AIJ), Vol. 80(716), (2015), pp. 887–896.

[4] Y. Tanaka, N. Hayashida, K. Masuda, S. Nishimura, T. Tanaka, Construction of experimental method for airflow analysis inside a soundproofing ventilation unit, International Journal of Emerging Engineering Research and Technology, Vol. 6(1), (2018), pp. 56-63.

[5] N. L. Phuong, K. Ito, S. Oonishi, S. Aramaki, Aerosol transport in vertical ventilation duct, part 1 – Experimental investigation of flow

field and aerosol transport in vertical duct with PIV method, Transactions of The Society of Heating, Air-Conditioning and Sanitary Engineers of Japan (SHASE), No. 179, (2012), pp. 35-42. (in Japanese)

[6] N. L. Phuong, K. Hirase, S. Aramaki, K. Ito, Flow field measurement in acrylic airway model by PIV and validation of CFD prediction results, Transactions of The Society of Heating, Air-Conditioning and Sanitary Engineers of Japan (SHASE), No. 207, (2014), pp. 1-7. (in Japanese)

[7] H. Kido, Y. Shiraishi, Unsteady CFD analysis to reduce calculation load of air flow field, Part 1 - Outline of calculation load reduction method and verification of prediction accuracy for constant air volume air-conditioning system, Transactions of The Society of Heating, Air-Conditioning and Sanitary Engineers of Japan (SHASE), No. 207, (2014), pp. 9-17. (in Japanese)

[8] DASSAULT SYSTEMES, TECHNICAL REFERENCE SOLIDWORKS FLOW SIMULATION 2014, pp. 1-3.

[9] DASSAULT SYSTEMES, SOLIDWORKS FLOW SIMULATION 2014, Online users guide, project: general setting: fluid flow: turbulent flow